

Proceedings of the 16th Czech and Slovak Conference on Magnetism, Košice, Slovakia, June 13–17, 2016

Structural and Thermomagnetic Properties of $\text{Fe}_{86-x}\text{Zr}_7\text{M}_x\text{Nb}_2\text{Cu}_1\text{B}_4$ ($\text{M} = \text{Co}, \text{Ni}, (\text{CoCr})$; $x = 0$ or 6) Amorphous Alloys

A. ŁUKIEWSKA*

Institute of Physics, Częstochowa University of Technology, Armii Krajowej 19, 42-200 Częstochowa, Poland

The effect of the substitution of Co, Ni or (CoCr) for the part of Fe atoms on the thermal stability and some magnetic properties, i.e. magnetization and magnetocaloric effect of $\text{Fe}_{86-x}\text{Zr}_7\text{M}_x\text{Nb}_2\text{Cu}_1\text{B}_4$ ($\text{M} = \text{Co}, \text{Ni}, (\text{CoCr})$; $x = 0$ or 6) alloys was investigated. From X-ray studies it was stated that the investigated alloys in the as-quenched state and after the accumulative annealing for 10 min at 600 K and then 700 K were fully amorphous. The amorphous as-quenched $\text{Fe}_{80}\text{Zr}_7\text{Ni}_6\text{Nb}_2\text{Cu}_1\text{B}_4$ alloy shows the lowest thermal stability and the onset of its crystallization temperature is equal to 775 K. The Arrott plots are almost linear and show positive slope near the Curie temperature. The maximum magnetic entropy change is very sensitive to the chemical composition and annealing conditions of the alloys.

DOI: [10.12693/APhysPolA.131.738](https://doi.org/10.12693/APhysPolA.131.738)

PACS/topics: 65.60.+a, 75.50.Kj, 75.50.Bb, 75.30.Sg

1. Introduction

In amorphous alloys based on transition metals various magnetic orderings such as paramagnetism, ferromagnetism superparamagnetism, superferromagnetism and spin glass, depending on compositions and method preparation, can be present [1]. The amorphous alloys represent metastable state and due to the structural relaxation their magnetic properties can be also distinctly modified by the proper annealing [2]. The relaxation process in the amorphous alloys occurs during annealing even at the relatively low temperature. Amorphous alloys containing transition metals have attracted great attention for over three decades [3] because they exhibit excellent soft magnetic properties. These alloys are interesting materials for fundamental studies and applications as well. The alloys with the Curie temperature close to room one are promising materials for magnetic refrigeration systems, because the magnetic entropy change, directly connected with the magnetocaloric effect, shows maximum near the temperature of the magnetic phase transition [4]. It is also worth noticing that the magnetic saturation of these amorphous alloys can be obtained at relatively low magnetic field.

The effect of the substitution of Co, Ni, or (CoCr) for the part of Fe atoms on the thermal stability and some magnetic properties, i.e. magnetization and magnetocaloric effect of $\text{Fe}_{86-x}\text{Zr}_7\text{M}_x\text{Nb}_2\text{Cu}_1\text{B}_4$ ($\text{M} = \text{Co}, \text{Ni}, (\text{CoCr})$; $x = 0$ or 6) alloys within amorphous state has been studied.

2. Experimental procedure

Master alloys $\text{Fe}_{86-x}\text{Zr}_7\text{M}_x\text{Nb}_2\text{Cu}_1\text{B}_4$ ($\text{M} = \text{Co}, \text{Ni}, (\text{CoCr})$; $x = 0$ or 6) have been prepared by arc-melting

of pure elements under a protective argon atmosphere. Obtained in this way ingots were remelted several times in order to achieve a good homogeneity. The amorphous ribbons 3 mm wide and 20 μm thick were produced by a rapid quenching method on a single roller. All investigations were performed for the samples in the as-quenched state and after the accumulative annealing in vacuum for 10 min at 600 K and then at 700 K. The annealing temperatures were chosen according to differential scanning calorimetry (DSC) curves recorded by NETSCH STA 449F1 Jupiter setup at the heating rate of 10 K/min. The microstructure of the investigated alloys was studied using a Bruker-AXS, type D8 Advanced X-ray diffractometer with Cu anode. The isothermal magnetization curves at magnetizing field induction in 0–1 T range were measured by VersaLab (Quantum Design) system for samples in the form of discs 3 mm in diameter cut out from ribbons. The step of measured temperature was equal to 5 K and its range was chosen according to the Curie temperature of the alloy.

3. Results and discussion

In Fig. 1 X-ray diffraction patterns of the samples annealed at 600 K for 10 min are depicted. In these patterns only broad maxima characteristic of amorphous materials are seen. The similar patterns were observed for as-quenched and annealed at 700 K samples.

Figure 2 shows the DSC curves measured at the heating rate 10 K/min in the temperature range from 300 K up to 1150 K for the as-quenched amorphous $\text{Fe}_{86-x}\text{Zr}_7\text{M}_x\text{Nb}_2\text{Cu}_1\text{B}_4$ ($\text{M} = \text{Co}, \text{Ni}, (\text{CoCr})$; $x = 0$ or 6) alloys. Distinct exothermic dips corresponding to the primary crystallization are observed in DSC curves. As can be seen from Fig. 2 replacement of 6 at.% Fe by Co or Ni in $\text{Fe}_{86}\text{Zr}_7\text{Nb}_2\text{Cu}_1\text{B}_4$ alloy shifts the onset of crystallization towards lower temperature because of thermal stability reduction of amorphous phase [5]. On the contrary to $\text{Fe}_{80}\text{Zr}_7\text{Co}_6\text{Nb}_2\text{Cu}_1\text{B}_4$ alloy the substitution of

*e-mail: aluk@wip.pcz.pl

3 at.% Co by Cr shifts the crystallization peak to the higher temperature because of amorphous structure stabilization [6]. The onset of the crystallization temperature estimated from DSC curves is equal to 801, 793, 775, and 808 K for $\text{Fe}_{86}\text{Zr}_7\text{Nb}_2\text{Cu}_1\text{B}_4$, $\text{Fe}_{80}\text{Zr}_7\text{Co}_6\text{Nb}_2\text{Cu}_1\text{B}_4$, $\text{Fe}_{80}\text{Zr}_7\text{Ni}_6\text{Nb}_2\text{Cu}_1\text{B}_4$, and $\text{Fe}_{80}\text{Zr}_7\text{Co}_3\text{Cr}_3\text{Nb}_2\text{Cu}_1\text{B}$, respectively. The peaks ascribed to the secondary crystallization are very broad and fuzzy (Fig. 2). It indicates that amorphous matrix in partially crystallized alloys is very inhomogeneous.

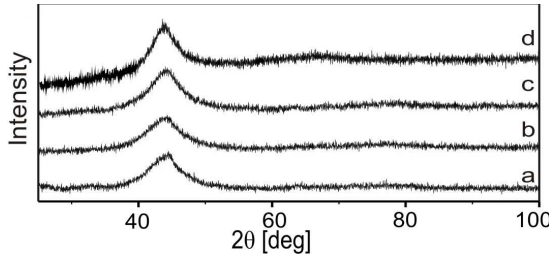


Fig. 1. X-ray diffraction patterns for the $\text{Fe}_{86-x}\text{Zr}_7\text{M}_x\text{Nb}_2\text{Cu}_1\text{B}_4$ alloys after annealing at 600 K for 10 min: $x = 0$ (a), $x = 6$, $M = \text{Co}$ (b), $x = 6$, $M = \text{Ni}$ (c), $x = 6$, $M = (\text{CoCr})$ (d).

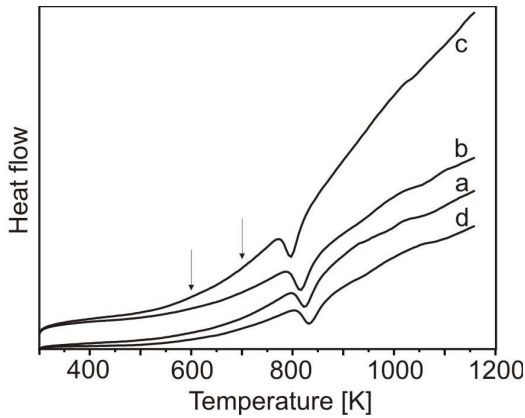


Fig. 2. DSC curves for $\text{Fe}_{86-x}\text{Zr}_7\text{M}_x\text{Nb}_2\text{Cu}_1\text{B}_4$ alloys in the as-quenched state: $x = 0$ (a); $x = 6$, $M = \text{Co}$ (b); $x = 6$, $M = \text{Ni}$ (c); $x = 6$, $M = (\text{CoCr})$ (d). Vertical arrows indicate the annealing temperatures of the samples.

The family of the isothermal magnetization curves ($\sigma(\mu_0 H)$) for $\text{Fe}_{86}\text{Zr}_7\text{Nb}_2\text{Cu}_1\text{B}_4$ alloy in the as-quenched state is presented in Fig. 3. Isothermal $\sigma(\mu_0 H)$ curves have been measured at various temperatures with the step of 5 K.

To determine the type of ferromagnetic-paramagnetic phase transition, the Arrott plots (Fig. 4) were constructed using the magnetization data. The positive slope of the Arrott plots near the Curie temperature indicates that the ferromagnetic-paramagnetic phase transition is of the second order type [7].

According to the thermodynamic theory, the isothermal magnetic entropy change (ΔS_M) corresponding to the variation of the magnetic field induction from 0 to

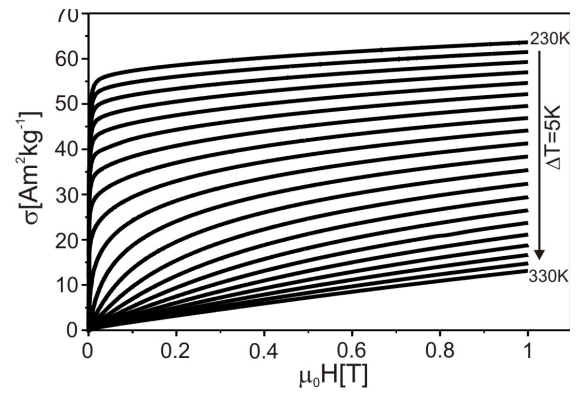


Fig. 3. Isothermal magnetization curves for the $\text{Fe}_{86}\text{Zr}_7\text{Nb}_2\text{Cu}_1\text{B}_4$ alloy in the as-quenched state in 230–330 K temperature range.

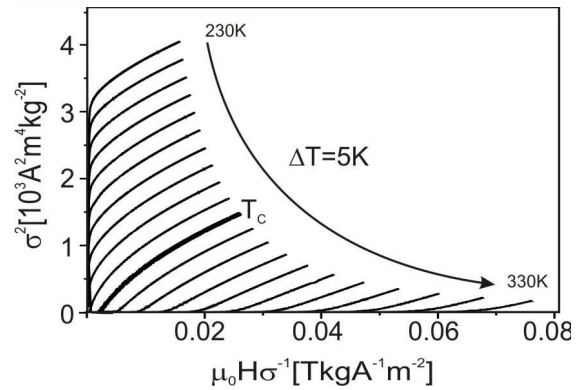


Fig. 4. Arrott plots i.e. σ^2 as a function of $\mu_0 H/\sigma$ for the $\text{Fe}_{86}\text{Zr}_7\text{Nb}_2\text{Cu}_1\text{B}_4$ alloy in the as-quenched state.

B_{\max} can be calculated from the Maxwell equation

$$\Delta S_M = \int_0^{B_{\max}} \left(\frac{\delta \sigma(T, B)}{\delta T} \right)_B dB, \quad (3.1)$$

where σ is the magnetization per unit mass, T — temperature, B — the magnetizing field induction and B_{\max} — maximum magnetizing field induction.

After approximation of the partial derivative in Eq. (3.1) by

$$\left(\frac{\delta \sigma(T, B)}{\delta T} \right)_B = \frac{\sigma(T_2, B) - \sigma(T_1, B)}{T_2 - T_1}, \quad (3.2)$$

the magnetic entropy change at temperature $\frac{T_1+T_2}{2}$ can be evaluated from the relation

$$\Delta S_M \left(\frac{T_1 + T_2}{2} \right) = \frac{1}{T_2 - T_1} \times \left[\int_0^{B_{\max}} \sigma(T_2, B) dB - \int_0^{B_{\max}} \sigma(T_1, B) dB \right] \quad (3.3)$$

where T_1 and T_2 are consecutive temperatures for which magnetization is measured [8]. The calculated values of $|\Delta S_M|$ versus temperature of as-quenched and annealed at 600 K for 10 min samples for maximum magnetizing field induction of $B_{\max} = 1$ T are depicted in Fig. 5.

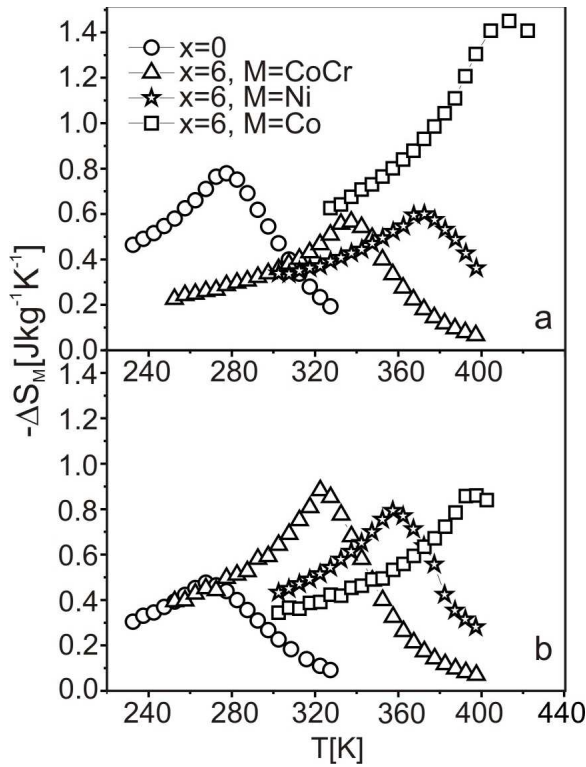


Fig. 5. The magnetic entropy change $|\Delta S_M|$ versus temperature for investigated alloys in the as-quenched state (a) and after the annealing at 600 K for 10 min (b).

TABLE I

Curie temperature (T_C) [9], the maximum magnetic entropy change ($|\Delta S_M|_{\max}$), the temperature of the maximum entropy change (T_{\max}) for the investigated alloys in the as-quenched state (asq) and after the accumulative annealing for 10 min at 600 K and then 700 K.

Sample	Heat treatment	T_C [K]	$ \Delta S_M _{\max}$ [J kg ⁻¹ K ⁻¹]	T_{\max} [K]
Fe ₈₆ Zr ₇ Nb ₂ B ₄ Cu ₁	asq	278	0.78	278
	600 K	272	0.48	268
	700 K	273	0.70	273
Fe ₈₀ Co ₆ Zr ₇ Nb ₂ B ₄ Cu ₁	asq	420	1.49	419
	600 K	396	0.86	396
	700 K	402	1.20	402
Fe ₈₀ Ni ₆ Zr ₇ Nb ₂ B ₄ Cu ₁	asq	374	0.60	373
	600 K	359	0.79	355
	700 K	360	0.99	350
Fe ₈₀ Co ₃ Cr ₃ Zr ₇ Nb ₂ B ₄ Cu ₁	asq	339	0.57	338
	600 K	326	0.88	323
	700 K	330	0.94	328

Some magnetic data determined from $|\Delta S_M| (T)$ curves are collected in Table I. As can be seen from Fig. 5a and Table I, the maximum $|\Delta S_M| (T)$ curve is the highest for the as-quenched Fe₈₀Zr₇Co₆Nb₂Cu₁B₄ alloy and is equal to 1.49 J/(kg K). After the annealing of the samples at 600 K for 10 min the maxima of the entropy change for

Fe₈₆Zr₇Nb₂Cu₁B₄ and Fe₈₀Zr₇Co₆Nb₂Cu₁B₄ alloys distinctly decrease (Fig. 5b, Table I) in comparison with the as-quenched state. As for Fe₈₀Zr₇Ni₆Nb₂Cu₁B₄ and Fe₈₀Zr₇Co₃Cr₃Nb₂Cu₁B₄ alloys, the increase of maximum entropy change after this heat treatment takes place (Fig. 5b, Table I).

Further heat treatment at 700 K for 10 min leads to the increase of the maximum entropy change of all investigated alloys as compared to the previous treatment (Table I). It is worth noticing that after the annealing the change of the temperature of this maximum is also observed (Fig. 5a,b, Table I). This is coincident with the Curie temperature change [9].

4. Conclusions

- In X-ray diffraction patterns of all samples broad maxima characteristic of amorphous alloys are only seen.
- As revealed by differential scanning calorimetry, after replacement of 6 at.% Fe by Co or Ni shifts the onset of crystallization to the lower temperature. However the substitution of 3 at.% Co by Cr stabilizes the amorphous structure which leads to the enhancement of crystallization temperature.
- The positive value of slope of the Arrott plots near the Curie temperature confirms a second order ferromagnetic–paramagnetic phase transition.
- Magnetic entropy change depends on the chemical composition of the investigated alloys and their thermal history.

References

- [1] J.M.D. Coey, *Amorphous Solid and the Liquid State* **13**, 433 (1985).
- [2] M.E. McHenry, M.A. Willard, D.E. Laughlin, *Progr. Mater. Sci.* **44**, 291 (1999).
- [3] G. Herzer, *Acta Mater.* **61**, 718 (2013).
- [4] J. Świerczek, A. Kupczyk, *J. Magn. Magn. Mater.* **386**, 74 (2015).
- [5] J. Torrens-Serra, P. Bruna, S. Roth, J. Rodriguez-Viejo, M.T. Clavaguera-Mora, *J. Alloys Comp.* **469**, 202 (2010).
- [6] L.M. Moreno-Ramirez, J.S. Blazquez, V. Franco, A. Conde, M. Marsilius, V. Budinsky, *J. Magn. Magn. Mater.* **409**, 56 (2016).
- [7] J. Mira, J. Rivas, F. Rivadulla, C. Vázquez-Vázquez, M.A. López-Quintela, *Phys. Rev. B* **60**, 2998 (1999).
- [8] J. Świerczek, *J. Magn. Magn. Mater.* **322**, 2696 (2010).
- [9] A. Łukiewska, J. Świerczek, M. Hasiak, J. Olszewski, J. Zbrozczyk, P. Gębara, W. Ciużyńska, *Nukleonika* **60**, 103 (2015).